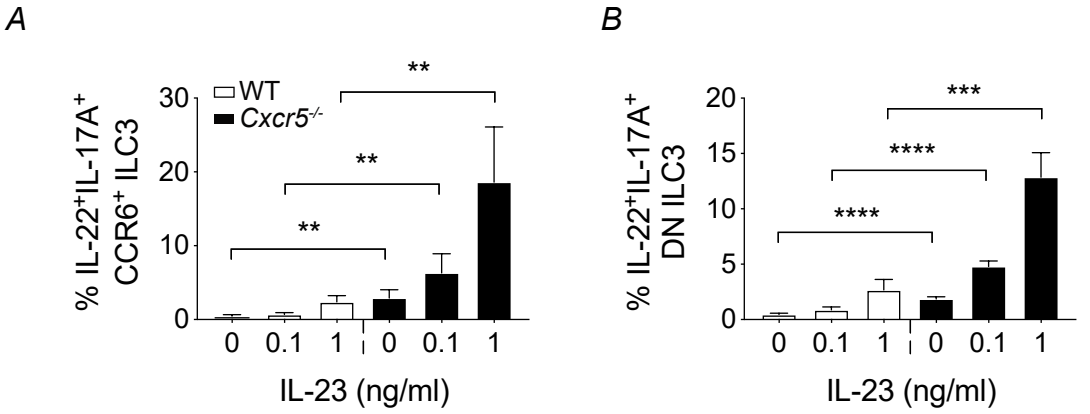


***SI Appendix*, Fig. S1.** Frequencies of *Cxcr5*$^{-/-}$ small intestine ILC3 that simultaneously produce IL-17A and IL-22 upon stimulation. Frequencies of IL-22- and IL-17A-double producing (*A*) LTi-like cells and (*B*) DN ILC3 after ex-vivo stimulation for 3 h with the indicated doses of IL-23 (n=4). Bar graphs show mean ± SEM. ** P<0.01, *** P<0.001 and **** P<0.0001 (unpaired Student's t-test). Data shown are representative of 3 independent experiments.

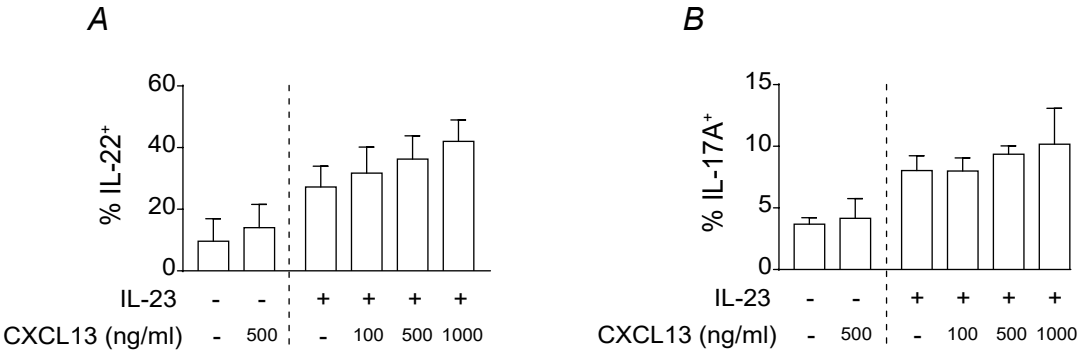


***SI Appendix*, Fig. S2.** CXCL13 does not directly suppress LTi-like cell cytokine production. Frequencies of (*A*) IL-22- and (*B*) IL-17A-producing small intestine LTi-like cells after ex-vivo stimulation with 1 ng/ml IL-23 in the presence of varying amounts of CXCL13, as indicated (n=3). Stimulations were carried out for 3 h. Bar graphs show mean ± SEM. Data shown are representative of 2 independent experiments.

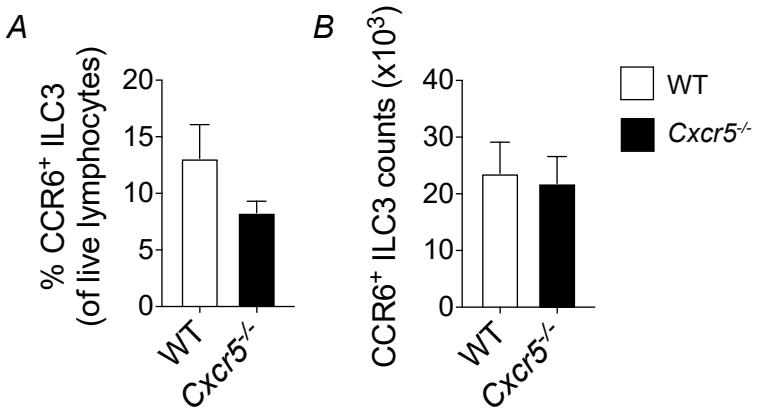


***SI Appendix*, Fig. S3.** Abundance of CCR6⁺ ILC3 in small intestines of *Cxcr5*$^{-/-}$ and WT neonates. (*A*) Frequencies and (*B*) absolute numbers of CCR6⁺ ILC3 in small intestines of *Cxcr5*$^{-/-}$ and WT control mice at postnatal day 0 (n=4). Bar graphs show mean ± SEM.

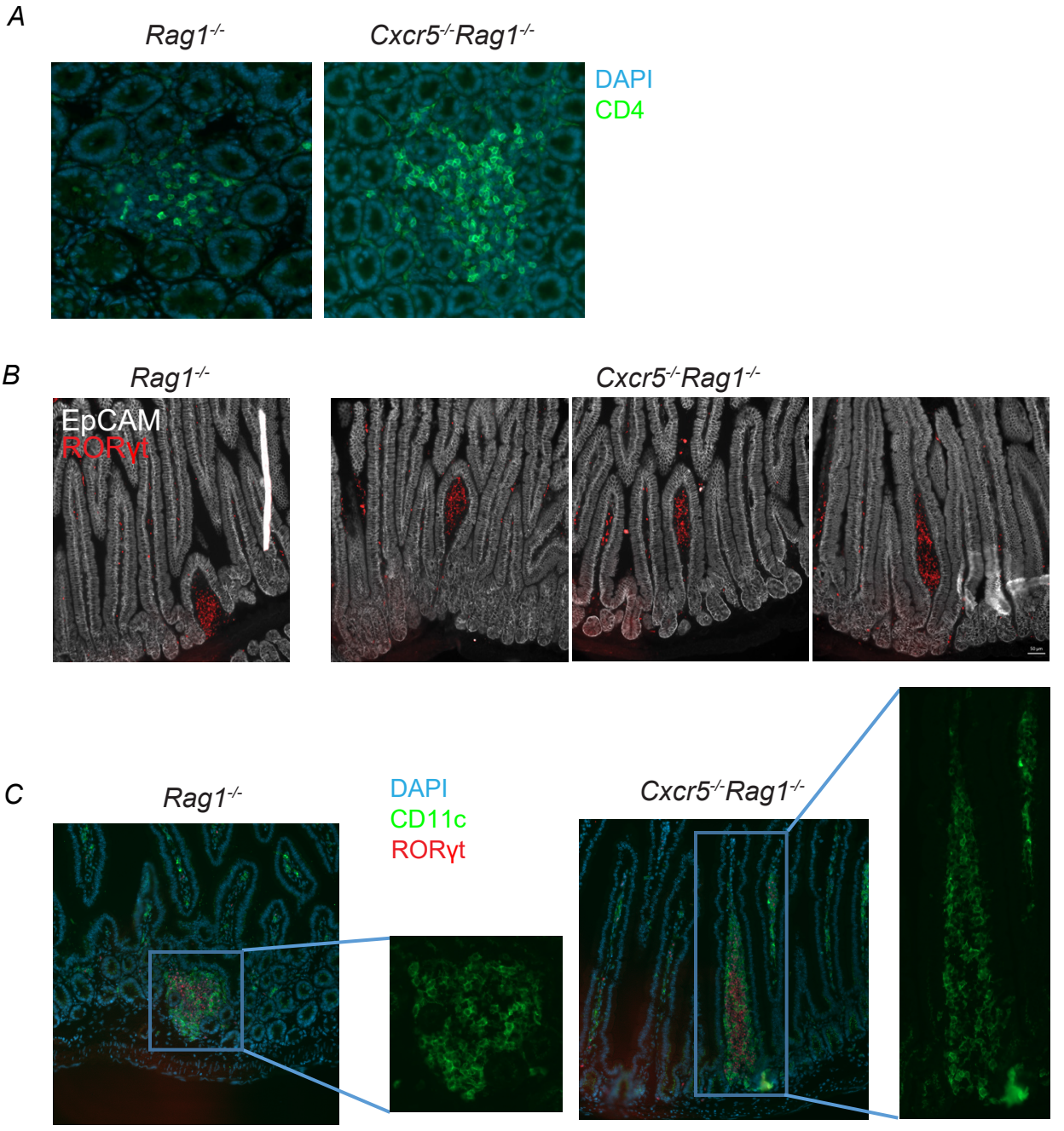


***SI Appendix*, Fig. S4.** Characterization of ileal SILT in *Cxcr5*$^{-/-}$*Rag1*$^{-/-}$ small intestines. (*A*) Representative images of crypt-level CD4$^{+}$ LTi-like cell aggregates in the distal small intestines of *Cxcr5*$^{-/-}$*Rag1*$^{-/-}$ and *Rag1*$^{-/-}$ control mice. (*B*) Representative images of villus RORγt$^{+}$ ILC3 aggregates in the proximal intestines of *Cxcr5*$^{-/-}$*Rag1*$^{-/-}$ and *Rag1*$^{-/-}$ control mice. (*C*) Representative images of CD11c$^{+}$ DCs in the proximal small intestines of *Cxcr5*$^{-/-}$*Rag1*$^{-/-}$ and *Rag1*$^{-/-}$ control mice. Insets from boxed areas show CD11c staining only. Tissue sections were stained with DAPI for nuclei labeling or EpCAM for epithelial cells visualization as indicated.

-

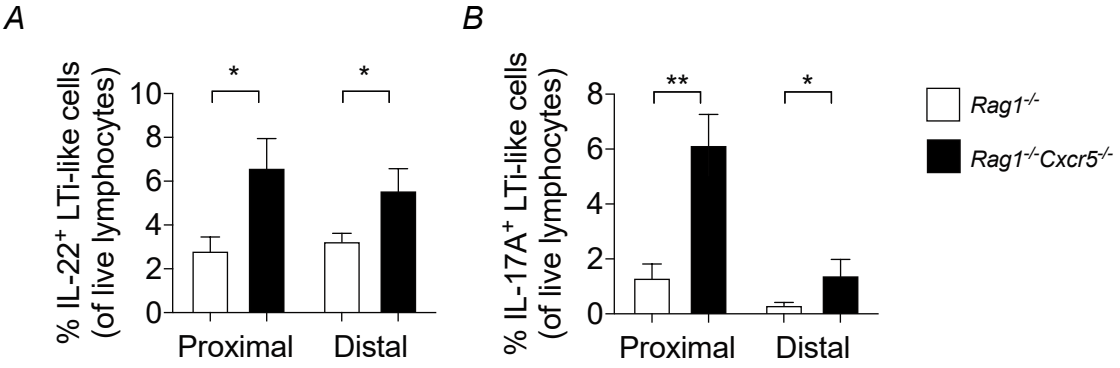


***SI Appendix*, Fig. S5.** Abundance of cytokine-producing LTi-like cells as a percentage of all live lymphocytes in proximal and distal areas of *Cxcr5*$^{-/-}$*Rag1*$^{-/-}$ and *Rag1*$^{-/-}$ small intestines. (*A*) IL-22- and (*B*) IL-17A-producing LTi-like cells expressed as a frequency of all small intestine live lymphocytes. Bar graphs show mean ± SD. * $P<0.05$ and ** $P<0.01$. Data shown are representative of 2 independent experiments.

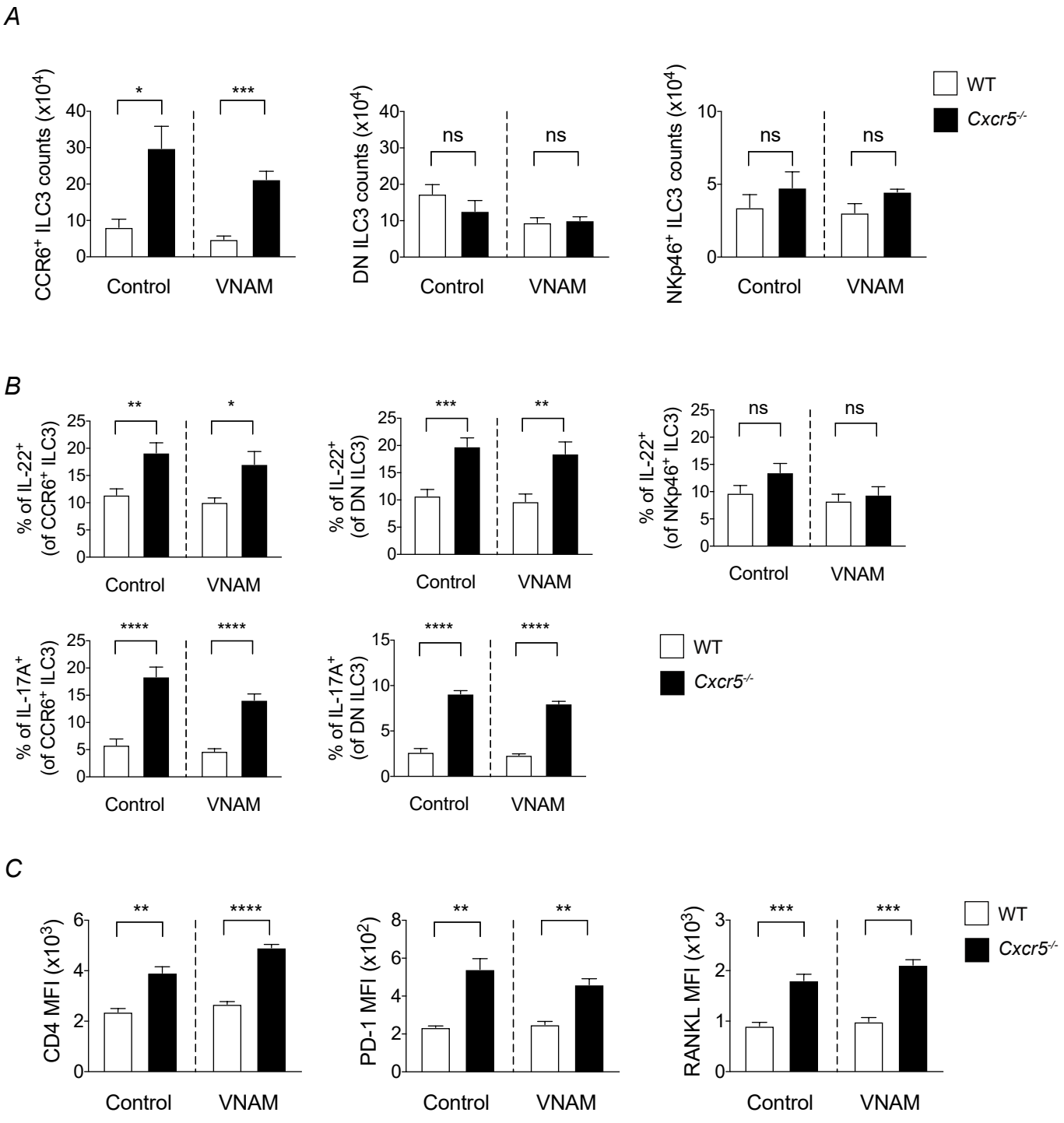


***SI Appendix*, Fig. S6.** Heightened LTi-like cell activity in *Cxcr5*$^{-/-}$ mice does not require microbio-ta-derived signals. (*A*) Total cell counts of small intestine LTi-like, DN and NKp46$^{+}$ ILC3 in *Cxcr5*$^{-/-}$ and WT mice that were administered VNAM or control drinking water for 4 weeks. (*B*) Frequen-cies of IL-22- and IL-17A-producing LTi-like, DN and NKp46$^{+}$ ILC3 from VNAM-treated or control mice after *ex vivo* stimulation with 1 ng/mL of IL-23. Stimulations were carried out for 3 h. (*C*) CD4, PD-1 and RANKL cell surface expression by LTi-like cells isolated from control or VNAM-treated *Cxcr5*$^{-/-}$ and WT mice. Bar graphs show mean ± SEM. * P<0.05, ** P<0.01, *** P<0.001 and **** P<0.0001. Data from *A* and *C* are representative of 2 independent experiments (n=3-4). Data in *B* were pooled from 2 independent experiments (n=7-8).